

VocalNet-MDM: Accelerating Streaming Speech LLM via Self-Distilled Masked Diffusion Modeling

Ziyang Cheng^{1,2*} Yuhao Wang^{1*} Heyang Liu^{1,2} Ronghua Wu² Qunshan Gu²
 Yanfeng Wang¹ Yu Wang^{1†}

¹Shanghai Jiao Tong University ²Ant Group

{colane, liuheyang, wangyanfeng622, yuwangsjtu, muye12}@sjtu.edu.cn
 {r.wu, guqunshan.gqs}@antgroup.com

Abstract

Recent Speech Large Language Models (LLMs) have achieved impressive capabilities in end-to-end speech interaction. However, the prevailing autoregressive paradigm imposes strict serial constraints, limiting generation efficiency and introducing exposure bias. In this paper, we investigate Masked Diffusion Modeling (MDM) as a non-autoregressive paradigm for speech LLMs and introduce VocalNet-MDM. To adapt MDM for streaming speech interaction, we address two critical challenges: training-inference mismatch and iterative overhead. We propose Hierarchical Block-wise Masking to align training objectives with the progressive masked states encountered during block diffusion decoding, and Iterative Self-Distillation to compress multi-step refinement into fewer steps for low-latency inference. Trained on a limited scale of only 6K hours of speech data, VocalNet-MDM achieves a $3.7 \times 10 \times$ decoding speedup and reduces first-chunk latency by 34% compared to AR baselines. It maintains competitive recognition accuracy while achieving state-of-the-art text quality and speech naturalness, demonstrating that MDM is a promising and scalable alternative for low-latency, efficient speech LLMs.

1 Introduction

Recent Speech LLMs have advanced end-to-end speech interaction through diverse multimodal architectures (Zeng et al., 2024; Xiaomi, 2025; Li et al., 2025; Wu et al., 2025a; Xu et al., 2025b; Wang et al., 2025c; Xu et al., 2025a). However, reliance on the Autoregressive (AR) paradigm limits real-time interaction. Latency grows linearly with sequence length due to serial dependence, and exposure bias degrades quality (Lin et al., 2025; Fan et al., 2025; Chen et al., 2025c). Despite various explorations to mitigate these issues (Long et al., 2025; Wang et al., 2025c,b; Bhati et al., 2025),

they remain within the AR framework, preventing substantial throughput improvements.

While non-autoregressive (NAR) generation offers a promising direction by predicting tokens in parallel to effectively reduce latency for real-time speech interaction and potentially benefiting from bidirectional context, current mainstream speech NAR paradigms still face significant limitations: single-pass methods based on conditional independence weaken long-range dependency modeling and global consistency (Fang et al., 2024; Luo et al., 2025); extra alignment components or supervision increase training complexity (Wang et al., 2024; Eskimez et al., 2024); and resolving the inherent one-to-many uncertainty in speech generation remains challenging, often requiring additional control signals (Liu et al., 2025a; Xin et al., 2024). These constraints motivate exploring an alternative NAR paradigm that retains parallel efficiency while addressing quality challenges.

In contrast, Masked Diffusion Modeling (MDM) offers a promising paradigm. Proven effective in large language models (Nie et al., 2025; Zhu et al., 2025b; Ye et al., 2025) and multimodal tasks (Yang et al., 2025b; You et al., 2025; Gong et al., 2025), MDM formulates generation as forward masking and reverse recovery, iteratively predicting masked tokens under updated contexts, forming globally consistent sequences without requiring extra alignment components. However, adapting MDM to streaming speech generation introduces two critical challenges. First, training-inference distribution mismatch: in streaming generation, MDM sequentially generates blocks of tokens by performing diffusion within each block and conditioning on previous blocks (Arriola et al., 2025). However, standard MDM adopts Global Bernoulli Masking (Nie et al., 2025), making blocks within the same sample appear similarly masked and mismatching block diffusion decoding, where past blocks are fully visible while the current block is progressively re-

vealed from fully masked to fully visible.

Second, cumulative latency from iterative refinement: to maintain generation quality, diffusion decoding still requires a number of denoising steps proportional to the sequence length, resulting in limited inference efficiency (Wu et al., 2025c; Chen et al., 2025d). Existing methods for accelerating iterative refinement also fall short. KV Cache adaptation improves overall throughput (Wu et al., 2025c; Ma et al., 2025; Hu et al., 2025) but cannot reduce first-chunk latency; distillation methods require complex multi-model coordination and incur high training costs on long speech sequences (Kim et al., 2025; Zhu et al., 2025c; Wu et al., 2025b).

Therefore, we explore a new paradigm for speech LLMs using MDM for speech generation, and introduce VocalNet-MDM, an MDM-based speech LLM. Our approach introduces two mechanisms. First, Hierarchical Block-wise Masking mitigates the training–inference mismatch in block diffusion decoding. Instead of Global Bernoulli Masking, it selects blocks and applies diverse intra-block masking ratios so that training covers the intermediate masked states encountered as each block is gradually denoised. Second, Iterative Self-Distillation reduces diffusion steps by using multi-step block refinement as self-supervision. It transfers more certain prediction distributions from later denoising steps to earlier steps via parallel updates across blocks, enabling few-step decoding while preserving multi-step quality.

Experiments demonstrate that VocalNet-MDM, trained on only 6K hours of data, achieves $3.7\times$ to over $10\times$ decoding speedup compared to the AR baseline and reduces first-chunk latency by 34%, while maintaining competitive WER and achieving state-of-the-art text quality and speech naturalness. These results validate MDM as a viable alternative to AR decoding and suggest a new, scalable direction for low-latency, efficient speech LLMs. Our key contributions are:

- **A new paradigm for speech LLMs via Masked Diffusion Modeling.** We systematically explore MDM in spoken dialogue and empirically validate its compatibility with NAR speech generation.
- **Hierarchical Block-wise Masking for training-inference alignment.** By explicitly covering progressive masked states in block diffusion decoding, we mitigate training-

inference mismatch and enhance generation quality under streaming inference.

- **Iterative Self-Distillation for low-latency inference.** We compress multi-step refinement into few-step decoding via parallel block-wise distillation, retaining multi-step quality without complex multi-model coordination.

2 Preliminary

Masked Diffusion Modeling. Masked diffusion language models define generation via a forward masking and a reverse recovery (Nie et al., 2025; Zhu et al., 2025a). Given a clean token sequence $\mathbf{s}_{1:T} \in \mathcal{V}^T$ and conditioning information \mathbf{c} , the forward process produces a partially masked sequence $\tilde{\mathbf{s}}$ by independently selecting a subset of positions to replace with a special mask token [MASK], while leaving the remaining tokens unchanged. Let $\mathcal{M} \subseteq \{1, \dots, T\}$ denote the set of masked positions in $\tilde{\mathbf{s}}$. The reverse process recovers the data by iteratively predicting the masked tokens.

The core component is a mask predictor $p_\theta(\cdot | \tilde{\mathbf{s}}, \mathbf{c})$, typically a Transformer without causal masking, which predicts all masked tokens in parallel conditioned on the partially observed sequence. Training minimizes the cross-entropy over masked positions:

$$\mathcal{L}(\theta) = \mathbb{E}_{\mathbf{s}, \mathbf{c}, \mathcal{M}} \left[\sum_{t \in \mathcal{M}} -\log p_\theta(s_t | \tilde{\mathbf{s}}, \mathbf{c}) \right], \quad (1)$$

where $\tilde{\mathbf{s}}$ is deterministically obtained from $(\mathbf{s}, \mathcal{M})$ by setting $\tilde{s}_t = M$ for $t \in \mathcal{M}$ and $\tilde{s}_t = s_t$ otherwise, and the expectation is taken over training samples (\mathbf{s}, \mathbf{c}) and masked sets \mathcal{M} drawn from a masking strategy. Unless otherwise specified, a common default is Global Bernoulli Masking, which samples a sequence-level masking ratio and then masks each position independently with this shared probability, spanning corruption levels from lightly masked inputs to highly masked sequences.

Decoding with Block Diffusion. In standard MDM decoding, one fixes a target length T , initializes $\tilde{\mathbf{s}}^{(0)} = [\text{MASK}]^T$, and iteratively predicts and updates masked tokens until all tokens are recovered (Zhu et al., 2025a). This whole-sequence denoising requires the full output canvas to be specified upfront, which is incompatible with streaming generation.

Block diffusion instead performs blockwise decoding: it generates blocks sequentially and denoises tokens within each block via masked diffusion (Arriola et al., 2025). Partition $\mathbf{s}_{1:T}$ into $K_{\text{blk}} = \lceil T/B \rceil$ contiguous blocks $\mathbf{s}^{(1)}, \dots, \mathbf{s}^{(K_{\text{blk}})}$ of size B . The induced model distribution factorizes as

$$p_{\theta}(\mathbf{s}_{1:T} \mid \mathbf{c}) = \prod_{k=1}^{K_{\text{blk}}} p_{\theta}(\mathbf{s}^{(k)} \mid \mathbf{s}^{(<k)}, \mathbf{c}). \quad (2)$$

Decoding proceeds sequentially for $k = 1, \dots, K_{\text{blk}}$: initialize the current block as $\tilde{\mathbf{s}}^{(k,0)} = M^B$, then simulate the reverse denoising process restricted to this block by iteratively applying the mask predictor conditioned on $\mathbf{s}^{(<k)}$ and \mathbf{c} , yielding a sample $\mathbf{s}^{(k)} \sim p_{\theta}(\mathbf{s}^{(k)} \mid \mathbf{s}^{(<k)}, \mathbf{c})$, which is appended to the prefix. Varying the block size interpolates between autoregressive decoding at $B = 1$ and whole-sequence diffusion when $K_{\text{blk}} = 1$.

3 Methodology

3.1 Overall Model Architecture

We develop VocalNet-MDM, a speech LLM that adopts the Thinker–Talker paradigm introduced by Qwen3-Omni (Xu et al., 2025b), as illustrated in Figure 1.

Given an input waveform \mathbf{x} , a Speech Encoder followed by a Downsample Adaptor produces a sequence of continuous representations $\mathbf{r}_{1:L}$. Conditioned on $\mathbf{r}_{1:L}$, the Thinker autoregressively generates the textual tokens $\mathbf{y}_{1:N}$ and outputs the corresponding hidden states $\mathbf{h}_{1:N}$:

$$\mathbf{y}_{1:N}, \mathbf{h}_{1:N} = \text{Thinker}(\mathbf{r}_{1:L}). \quad (3)$$

The Talker generates a discrete speech token sequence $\mathbf{s}_{1:T}$ of length T . Since typically $T \gg N$, we apply intra-block sparse semantic anchor alignment to construct $\mathbf{h}'_{1:T}$ from $\mathbf{h}_{1:N}$. Specifically, we partition the speech timeline into blocks of size B and place semantic anchors at the first Q positions of each block, setting all other positions to 0. Anchor semantics are assigned in an order-preserving, prefix-only manner to avoid future semantic leakage. Details are provided in Appendix B.1.

During training, the Talker processes a corrupted input sequence $\tilde{\mathbf{s}}_{1:T}$, obtained by masking $\mathbf{s}_{1:T}$ with [MASK] token. Its embedding sequence is denoted as $\mathbf{E}_{1:T}^s = \text{Embed}(\tilde{\mathbf{s}}_{1:T})$. We add the speech embeddings to the aligned semantics and apply a two-

layer feed-forward Fusion module:

$$\begin{aligned} \mathbf{u}_{1:T} &= \text{ReLU}(\mathbf{W}_1(\mathbf{E}_{1:T}^s + \mathbf{h}'_{1:T}) + \mathbf{b}_1), \\ \mathbf{e}_{1:T} &= \mathbf{W}_2 \mathbf{u}_{1:T} + \mathbf{b}_2. \end{aligned} \quad (4)$$

The fused features $\mathbf{e}_{1:T}$ are fed into the Talker, which performs MDM to conditionally predict the masked speech tokens. Finally, the predicted discrete speech tokens are converted into waveforms using the pretrained flow matching model and the HiFi-GAN vocoder from CosyVoice2 (Du et al., 2024), enabling high fidelity and low latency streaming speech reconstruction.

3.2 Masked Diffusion Modeling

Talker adopts the non-autoregressive MDM paradigm (Figure 1(a)). Given the fused feature sequence $\mathbf{e}_{1:T}$, the Talker predicts masked positions in parallel under a conditional independence approximation, instantiating an intra-block parallel, inter-block causal modeling scheme.

Block-Causal Attention Mechanism. To enable streaming generation, we adopt Block-Causal attention (Arriola et al., 2025). We divide a length- T sequence into consecutive blocks of size B . Tokens within the same block are fully visible to each other, enabling parallel computation within the block. Across blocks, attention is restricted causally: each token can attend to all positions in the current block and all preceding blocks, ensuring strict inter-block causality.

Masking Strategies. To support MDM training, we adopt Global Bernoulli Masking (Nie et al., 2025) where each token is independently masked with probability $\gamma_g \sim U(\gamma_g^{\min}, \gamma_g^{\max})$, providing uniform training signals across all positions. However, to better align training with the intermediate patterns encountered during block diffusion decoding, we propose a Hierarchical Blockwise Masking strategy. By hierarchically sampling masking ratios, this approach explicitly covers the progressive states where blocks transition from fully masked to fully visible, thereby bridging the training-inference distribution gap. Figure 2 illustrates the two masking strategies.

Concretely, for each sample we partition the valid speech token indices into $K_{\text{blk}} = \lceil T/B \rceil$ consecutive blocks, where the index set of the k -th block is

$$\begin{aligned} \mathcal{I}_k &= \{t \mid (k-1)B < t \leq \min(kB, T)\}, \\ k &= 1, \dots, K_{\text{blk}}. \end{aligned} \quad (5)$$

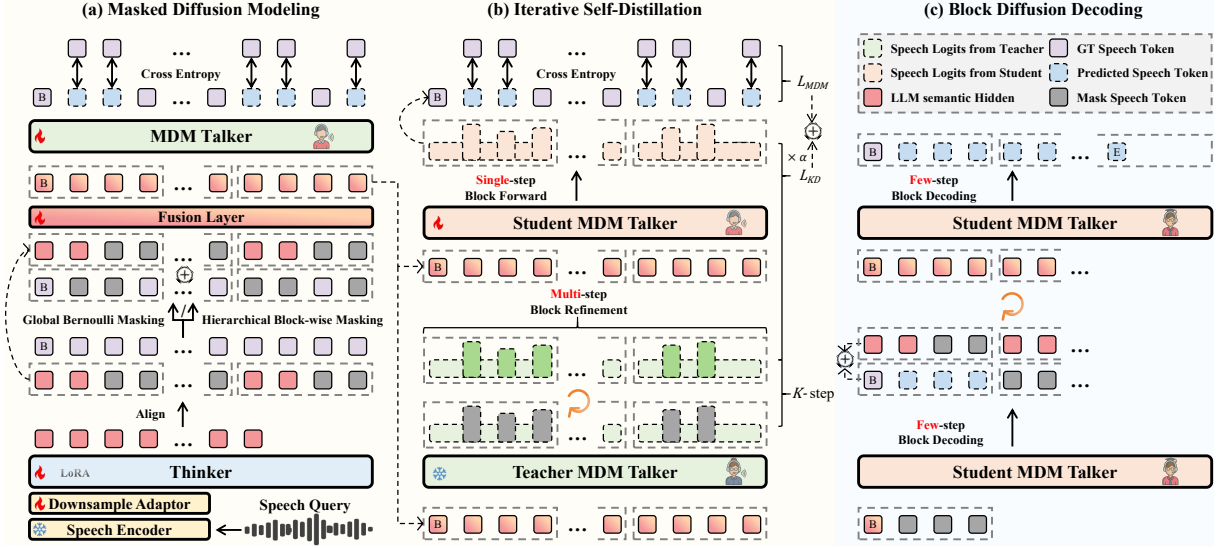


Figure 1: **Overview of our approach.** (a) Masked Diffusion Modeling: a Thinker–Talker speech LLM architecture where speech generation is performed via MDM. (b) Iterative Self-Distillation: transferring more certain distributions from later to earlier denoising steps to enable few-step inference. (c) Block Diffusion Decoding: streaming inference that denoises tokens within fixed-size blocks over diffusion steps.

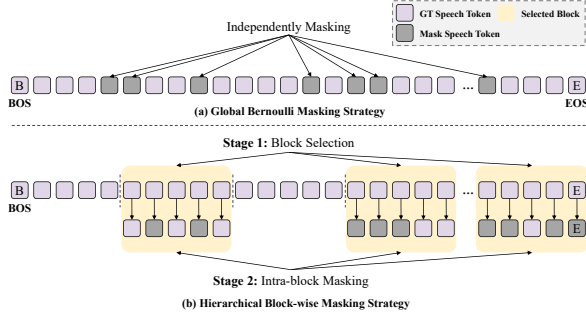


Figure 2: **Masking strategies.** (a) Global Bernoulli Masking: each token masked independently with uniform probability. (b) Hierarchical Block-wise Masking: block selection followed by intra-block token masking.

Masking is sampled via a two-stage randomized process: we first select a random subset of blocks $\mathcal{K}_{\text{mask}}$ based on a block-level ratio $\gamma_c \sim U(\gamma_c^{\min}, \gamma_c^{\max})$, then within each selected block we mask a fraction of positions determined by $\gamma_t \sim U(\gamma_t^{\min}, \gamma_t^{\max})$ to form \mathcal{M} . The complete algorithmic procedure is provided in Appendix B.2.

MDM Training Objective. Given the masked set \mathcal{M} , the corrupted input $\tilde{s}_{1:T}$, and the aligned semantic stream $\mathbf{h}'_{1:T}$, we minimize the cross-entropy loss on masked positions:

$$\mathcal{L}_{\text{MDM}} = - \sum_{t \in \mathcal{M}} \log P(s_t | \tilde{s}_{1:T}, \mathbf{h}'_{1:T}) . \quad (6)$$

3.3 Accelerated Inference via Iterative Self-Distillation

Although MDM alleviates the serial bottleneck of autoregressive decoding via parallel prediction, high-quality speech typically relies on multi-step iterative unmasking, which incurs additional latency. To balance quality and latency, we propose Iterative Self-Distillation (Figure 1(b)), distilling the teacher’s more confident predictions from later denoising steps into earlier ones, enabling few-step inference while preserving multi-step quality.

During training, the Teacher is a frozen replica of the model, and the Student is optimized with distillation targets. The Teacher runs K iterations of MDM and dynamically collects supervision signals to construct a target tensor \mathbf{Z}_{tea} .

Block-wise Teacher Update. Given the corrupted training input $\tilde{s}_{1:T}^{(0)}$ and its masked set \mathcal{M} , at iteration j ($1 \leq j \leq K$) the Teacher produces logits $\mathbf{z}_{\text{tea}}^{(j)}(t)$ conditioned on the current sequence $\tilde{s}_{1:T}^{(j-1)}$ and the semantic stream $\mathbf{h}'_{1:T}$. We adopt a block-wise update strategy with parallel updates across blocks: within each block of size B , we independently reveal a subset of masked positions based on confidence. This avoids inefficient global ranking and block-by-block serial updates. For position t , we define the confidence as

$$u_t^{(j)} = \max_{v \in \mathcal{V}} \text{Softmax} \left(\mathbf{z}_{\text{tea}}^{(j)}(t) \right)_v . \quad (7)$$

For each block, at iteration j we select the top- n_j masked positions with relatively highest confidence within the block and replace their [MASK] tokens with argmax predictions, yielding $\tilde{\mathbf{s}}^{(j)}$.

Update Scheduling and Dynamic Logit Collection. Let R_j denote the number of remaining masked positions in a given block at the beginning of iteration j . The number of updates n_j is determined by an even-allocation schedule:

$$r_j = K - j + 1, \quad n_j = \begin{cases} 0, & R_j = 0, \\ \left\lceil \frac{R_j}{r_j} \right\rceil, & \text{otherwise.} \end{cases} \quad (8)$$

When a position t is revealed at iteration j , we record the Teacher logits at that moment as its distillation target:

$$\mathbf{Z}_{\text{tea}}(t) = \mathbf{z}_{\text{tea}}^{(j)}(t), \quad \forall t \in \mathcal{U}^{(j)}, \quad (9)$$

where $\mathcal{U}^{(j)}$ denotes the set of positions revealed at iteration j .

Distillation Objective. The Student produces logits $\mathbf{z}_{\text{stu}}(t)$ in a single forward pass and matches the Teacher target tensor \mathbf{Z}_{tea} . We adopt Reverse KL with temperature τ as the distillation loss:

$$\mathcal{L}_{\text{KD}} = \frac{\tau^2}{|\mathcal{M}|} \sum_{t \in \mathcal{M}} \text{KL} \left(\text{Softmax}(\mathbf{z}_{\text{stu}}(t)/\tau) \parallel \text{Softmax}(\mathbf{Z}_{\text{tea}}(t)/\tau) \right). \quad (10)$$

The final objective is a weighted combination of the distillation loss and the original masked cross-entropy:

$$\mathcal{L}_{\text{Distill}} = \alpha \mathcal{L}_{\text{KD}} + (1 - \alpha) \mathcal{L}_{\text{MDM}}. \quad (11)$$

Training Strategy. The training proceeds in three progressive stages. We first align the Thinker to the audio modality using speech-to-text data via LoRA. We then train the Talker with \mathcal{L}_{MDM} using Global Bernoulli masking to establish parallel prediction. Finally, we fine-tune the Talker with $\mathcal{L}_{\text{Distill}}$ using Hierarchical Block-wise Masking.

3.4 Block Diffusion Decoding

To enable low-latency interaction, we generate speech in consecutive fixed-size blocks of length B using Block Diffusion Decoding (Figure 1(c)). Given a prefix $\mathbf{s}_{<t_0}$, we initialize the the subsequent block with [MASK] and denoise it for K diffusion steps. At each step j , the Talker predicts

distributions for masked positions conditioned on \mathbf{h}' and $\mathbf{s}_{<t_0}$, computes confidence via Eq. (7), and unmasks the top- n_j tokens following Eq. (8). The resulting block is then appended to the prefix for the next iteration; if an EOS token is generated, we truncate the sequence at the earliest EOS and terminate generation.

4 Experiments

4.1 Experimental Setup

Datasets. We follow the data construction protocol of VocalNet (Wang et al., 2025c), combining VoiceAssistant-400K from Mini-Omni and Ultra-Chat from SLAM-Omni (Xie and Wu, 2024; Chen et al., 2025b). VoiceAssistant-400K is generated by GPT-4o, yielding approximately 430K single-turn query-response pairs. UltraChat is split from multi-round dialogues into single-turn interactions, producing roughly 300K samples. Speech responses are synthesized via CosyVoice2-0.5B (Du et al., 2024), and we use its corresponding discrete codec tokens for training and decoding. The training set totals around 730K examples, corresponding to approximately 6k hours of speech.

Model Configuration. We use Whisper-large-v3 (Radford et al., 2023) with $5 \times$ downsampling as the speech encoder. The Thinker is initialized from Qwen3-8B (Yang et al., 2025a). The Talker shares a similar architectural design with the Thinker but uses 4 Transformer layers and is trained separately from scratch. The AR baselines share the same architecture and train the Talker autoregressively with next-token prediction (NTP) and multi-token prediction (MTP), where MTP follows Wang et al. (2025c).

Training Details. We set the block size, distillation iterations, and semantic anchors to $B = 16$, $K = 4$, and $Q = 4$, respectively. Global Bernoulli masking probability is sampled from $[\gamma_g^{\min}, \gamma_g^{\max}] = [0.3, 0.8]$. For Hierarchical Block-wise Masking, block-level ratio is sampled from $[\gamma_c^{\min}, \gamma_c^{\max}] = [0.5, 1.0]$, and intra-block ratio from $[\gamma_t^{\min}, \gamma_t^{\max}] = [0.3, 1.0]$. We use temperature $\tau = 2.0$ and weight $\alpha = 0.7$. Distillation uses a frozen teacher, adding only forward refinements.

We use AdamW with learning rate 2×10^{-4} and batch size 32 on A100 GPUs. We train the Thinker and downsampling adapter for 1 epoch, the Talker for 8 epochs with \mathcal{L}_{MDM} using Global Bernoulli Masking. For distillation fine-tuning,

Model	Efficiency		Text Quality				Speech Quality		
	TPS↑	RTF↓	AlpacaEval	Llama Q.	TriviaQA	Web Q.	Avg	WER↓	UTMOS↑
SLAM-Omni (Chen et al., 2025b)	61.13	0.8180	3.50	2.94	0.39	0.84	1.92	5.78	4.46
VITA-Audio (Long et al., 2025)	64.62	0.1934	6.93	7.43	4.27	5.23	5.96	3.83	4.26
GLM-4-Voice (Zeng et al., 2024)	39.06	0.3200	5.86	7.74	4.95	5.56	6.03	11.90	4.23
MiniCPM-o (OpenBMB, 2025)	212.16	0.2205	6.13	7.72	6.43	7.16	6.86	9.52	4.14
Qwen2.5-Omni (Xu et al., 2025a)	58.82	0.8484	6.01	7.90	5.89	6.88	6.67	2.31	4.34
Kimi-Audio (Ding et al., 2025)	30.77	0.4062	6.49	8.10	6.15	7.10	6.96	14.71	2.87
VocalNet-8B (Wang et al., 2025c)	374.81	0.0667	7.12	7.95	6.24	6.48	6.95	3.64	4.49
MiMo-Audio (Xiaomi, 2025)	476.51	0.4197	7.35	7.70	4.90	5.80	6.44	6.13	3.68
Baseline-AR (NTP)	204.64	0.1222	7.43	8.27	6.15	6.42	7.07	10.66	4.48
Baseline-AR (MTP)	374.81	0.0667	7.43	8.27	6.15	6.42	7.07	4.05	4.49
VocalNet-MDM (Step 16)	221.58	0.1128	7.43	8.27	6.15	6.42	7.07	5.53	4.49
VocalNet-MDM (Step 8)	390.72	0.0639	7.43	8.27	6.15	6.42	7.07	5.55	4.49
VocalNet-MDM (Step 4)	757.58	0.0329	7.43	8.27	6.15	6.42	7.07	5.34	4.49
VocalNet-MDM (Step 2)	1327.80	0.0188	7.43	8.27	6.15	6.42	7.07	6.10	4.47
VocalNet-MDM (Step 1)	2153.43	0.0116	7.43	8.27	6.15	6.42	7.07	6.23	4.46

Table 1: Comparison of VocalNet-MDM with open-source speech LLMs and an autoregressive baseline (Baseline-AR). Baseline-AR uses the same backbone as VocalNet-MDM and differs only in the talker, using next-token prediction (NTP) or multi-token prediction (MTP), whereas VocalNet-MDM uses masked diffusion modeling (MDM). **Bold** indicates the best performance. Gray entries denote metrics shared across variants.

we create a frozen copy of this checkpoint as the teacher and continue training the Talker for 4 epochs with $\mathcal{L}_{\text{Distill}}$ using Hierarchical Block-wise Masking. The frozen teacher performs only forward refinements without parameter updates.

Evaluation. We evaluate on the English subsets of OpenAudioBench (Li et al., 2025): AlpacaEval (Li et al., 2023), Llama Questions (Nachmani et al., 2023), TriviaQA (Joshi et al., 2017), and Web Questions (Berant et al., 2013). Text quality is scored by Qwen-max for correctness and relevance on a 0–10 scale. See Appendix D for details. Speech quality is measured by UTMOS (Saeki et al., 2022) for naturalness and WER using Whisper-large-v3 transcriptions for speech-text alignment.

We report efficiency using TPS and RTF, defined as generated speech tokens divided by inference latency, and inference latency divided by speech duration, respectively. Latency is measured for speech token generation only. For aligned multimodal models, we measure Talker latency; for native multimodal models, we measure speech-token generation latency in the unified model. Token counting includes only speech tokens. All measurements are conducted on a single L20 GPU.

4.2 Main Results

Table 1 compares VocalNet-MDM with open-source speech LLMs and an autoregressive baseline (Baseline-AR) in terms of efficiency, text quality,

and speech quality. For VocalNet-MDM, Step K denotes K diffusion steps per block.

Text Quality. VocalNet-MDM achieves the best average text quality score of 7.07. Specifically, it obtains 7.43 on AlpacaEval and 8.27 on Llama Questions, both representing the highest scores across all models, demonstrating that our approach preserves the strong semantic understanding and reasoning capabilities of the Qwen3-8B base model. On TriviaQA and Web Questions, VocalNet-MDM achieves 6.15 and 6.42 respectively, ranking third. Overall, VocalNet-MDM demonstrates balanced performance across all four evaluation datasets, achieving the best comprehensive text quality.

Efficiency Advantages. VocalNet-MDM demonstrates substantial efficiency advantages over both AR baselines and open-source models. Relative to Baseline-AR (NTP), Step 4 improves TPS by $3.7\times$ and reduces RTF by 73%, while Step 1 achieves even more dramatic gains with $10.5\times$ higher TPS and 90.5% RTF reduction. Relative to Baseline-AR (MTP), Step 4 achieves $2.0\times$ higher TPS, and Step 1 delivers $5.7\times$ speedup. Among prior models, Step 4 attains $1.6\times$ higher TPS than the second-fastest model, MiMo-Audio, while Step 1 achieves $4.5\times$ higher TPS. The RTF of Step 4 and Step 1 are also markedly lower than most open-source models, which typically exceed 0.4.

Speech Quality. VocalNet-MDM maintains competitive speech quality across configurations.

Model	First chunk latency (ms)↓
SLAM-Omni	742.32 ± 38.22
VITA-Audio	512.64 ± 33.55
GLM-4-Voice	1066.02 ± 21.78
MiniCPM-o	1329.52 ± 257.27
Qwen2.5-Omni	N/A
Kimi-Audio	1371.48 ± 137.50
VocalNet-8B	462.32 ± 45.07
MiMo-Audio	N/A
Baseline-AR (NTP)	555.86 ± 17.88
Baseline-AR (MTP)	481.22 ± 19.58
VocalNet-MDM (Step 1)	368.67 ± 13.82
VocalNet-MDM (Step 2)	373.29 ± 14.00
VocalNet-MDM (Step 4)	382.36 ± 14.34
VocalNet-MDM (Step 8)	402.19 ± 15.08
VocalNet-MDM (Step 16)	427.45 ± 16.25

Table 2: First-chunk latency reported as mean ± standard deviation. N/A indicates models without official streaming inference implementations, for which first-chunk latency cannot be measured.

Step 16, 8, 4, 2, and 1 all achieve UTMOS scores of 4.49, 4.49, 4.49, 4.47, and 4.46 respectively, with Step 4 through 16 exceeding all other models in naturalness. For speech–text alignment, Step 1 through 4 achieve WER ranging from 5.34 to 6.23, substantially improving over Baseline-AR (NTP) at 10.66 and approaching Baseline-AR (MTP) at 4.05. Compared to other models, Step 4 outperforms SLAM-Omni (5.78), MiMo-Audio (6.13), MiniCPM-o (9.52), GLM-4-Voice (11.90), and Kimi-Audio (14.71), while Step 1 maintains competitive performance with WER of 6.23.

Efficiency–Quality Trade-off. VocalNet-MDM offers flexible operating points to balance efficiency and quality. Step 4 serves as a strong default: it matches Step 16 in naturalness with an identical UTMOS of 4.49, maintains a low WER of 5.34, and incurs lower training cost. We therefore adopt $K = 4$ as the default distillation iteration count. Step 1 targets latency-critical settings, achieving the highest throughput of 2153.43 TPS and lowest RTF of 0.0116 while preserving competitive quality with WER 6.23 and UTMOS 4.46.

4.3 Detailed Efficiency Analysis

We evaluate first-chunk latency and its components in streaming generation scenarios on a single L20 GPU. For models lacking official streaming implementations, or with adjustable parameters, we standardize the speech chunk length to approximately 0.6 seconds to ensure fair comparison. For models

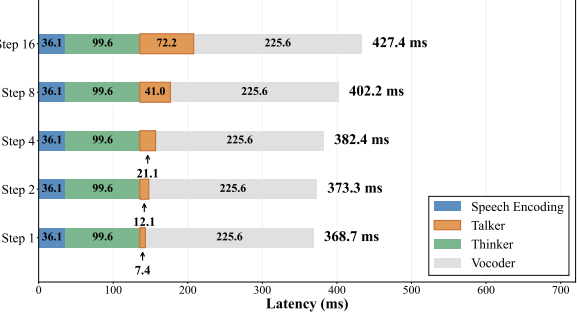


Figure 3: Latency breakdown for generating the first-chunk in VocalNet-MDM at different diffusion steps.

with officially recommended streaming configurations, we adhere to their prescribed settings.

Table 2 presents first-chunk latency comparison. VocalNet-MDM achieves the lowest latency across all configurations. Step 1 attains the optimal latency of 368.67ms. Compared to higher-latency models where GLM-4-Voice, MiniCPM-o, and Kimi-Audio exhibit 1066.02ms, 1329.52ms, and 1371.48ms respectively, our Step 16 achieves only 427.45ms, delivering over 2× reduction.

Figure 3 further illustrates the latency breakdown of VocalNet-MDM. All configurations maintain consistent latency across Speech Encoding, Thinker, and Vocoder modules at 36.1ms, 99.6ms, and 225.6ms respectively. The Talker module latency decreases with fewer diffusion steps, from 72.2ms at Step 16 to 7.4ms at Step 1. Vocoder latency is dominated by flow matching, which is not essential to the vocoder architecture (Xiaomi, 2025; Wang et al., 2025b). We therefore leave vocoder optimization out of scope.

4.4 Impact of Masking Strategy

We compare masking strategies with identical distillation configurations $\alpha = 0.7$ and $\tau = 2.0$ (Table 3). Without distillation, Hierarchical Block-wise Masking exhibits higher WER of 10.43, 15.38, and 50.70 at Step 4, 2, and 1, while Global Bernoulli masking achieves lower WER of 6.75, 9.95, and 39.00. This shows Hierarchical Block-wise Masking struggles to establish parallel prediction capabilities without iterative refinement guidance, while Global Bernoulli masking provides uniform training signals suitable for this purpose.

With Iterative Self-Distillation, switching to Hierarchical Block-wise Masking during fine-tuning reduces WER from 7.65 to 5.34 at Step 4 and from 9.69 to 6.23 at Step 1, representing 30% and 36% relative improvements respectively, while maintain-

MDM Training Masking Strategy	Distillation FT Masking Strategy	Step 4		Step 2		Step 1	
		WER↓	UTMOS↑	WER↓	UTMOS↑	WER↓	UTMOS↑
Hierarchical Block-wise Masking	N/A	10.43	4.46	15.38	4.41	50.70	3.84
Global Bernoulli Masking	N/A	6.75	4.47	9.95	4.42	39.00	3.87
Global Bernoulli Masking	Global Bernoulli Masking	7.65	4.46	7.91	4.45	9.69	4.42
Global Bernoulli Masking	Hierarchical Block-wise Masking	5.34	4.49	6.10	4.47	6.23	4.46

Table 3: Ablation study on masking strategies. MDM Training Masking Strategy denotes the masking strategy used to train the Talker with \mathcal{L}_{MDM} . Distillation FT Masking Strategy denotes the masking strategy used during self-distillation fine-tuning with $\mathcal{L}_{\text{Distill}}$, and N/A indicates that the distillation fine-tuning stage is omitted. The best results are highlighted in **bold**.

α	τ	Step 4		Step 2		Step 1	
		WER↓	UTMOS↑	WER↓	UTMOS↑	WER↓	UTMOS↑
N/A	N/A	6.75	4.47	9.95	4.42	39.00	3.87
0.7	2.0	5.34	4.49	6.10	4.47	6.23	4.46
0.0	N/A	6.29	4.47	9.77	4.43	41.27	3.86
0.9	2.0	10.07	4.46	10.03	4.44	15.95	4.32
0.7	1.0	5.95	4.48	6.55	4.47	9.55	4.42
0.7	3.0	5.73	4.49	6.20	4.46	9.26	4.41

Table 4: Performance under different self-distillation hyperparameter settings. The row with N/A indicates the model trained without the distillation fine-tuning stage. The best results are highlighted in **bold**.

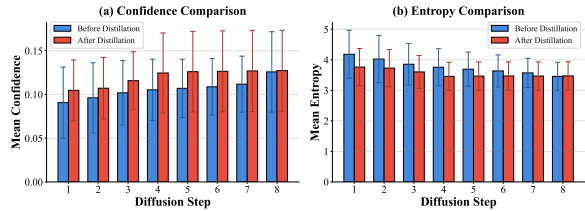


Figure 4: Comparison of prediction uncertainty before and after Iterative Self-Distillation. (a) Mean confidence scores across diffusion steps. (b) Mean entropy values across diffusion steps.

ing UTMOS scores of 4.49 and 4.46. Hierarchical Block-wise Masking better simulates the intermediate states during block diffusion decoding, enabling more effective compression of multi-step refinement into fewer inference steps. This validates our two-stage training pipeline: first establishing parallel prediction capabilities with Global Bernoulli masking, then switching to Hierarchical Block-wise Masking to align training states with block diffusion decoding patterns.

4.5 Impact of Iterative Self-Distillation

Hyperparameter Analysis. We analyze the impact of distillation loss weight α and temperature τ on performance (Table 4). Without distillation ($\alpha = 0$), WER reaches 6.29 and 41.27 at Step 4 and Step 1, compared to 5.34 and 6.23 under $\alpha = 0.7$ and $\tau = 2.0$. This indicates the effectiveness of It-

erative Self-Distillation in compressing multi-step refinement. However, excessive distillation weight ($\alpha = 0.9$) degrades performance, indicating the need to balance teacher guidance with ground-truth supervision. For temperature, $\tau = 2.0$ consistently outperforms $\tau = 1.0$ and $\tau = 3.0$, as extreme values produce teacher distributions that are either overly sharp or overly smooth. Thus, we adopt $\alpha = 0.7$ and $\tau = 2.0$ as our default configuration.

Uncertainty Reduction Analysis. We further examine how distillation accelerates convergence by measuring prediction uncertainty through mean confidence and entropy. As shown in Figure 4, distillation substantially reduces uncertainty at early diffusion steps: Step 1 and 2 achieve similar confidence and entropy levels comparable to baseline Step 4, while Step 4 reaches performance matching baseline Step 8. These findings demonstrate that Iterative Self-Distillation effectively transfers the uncertainty resolution process from later steps to earlier ones, enabling few-step generation to match the quality of multi-step generation.

5 Conclusion

This work systematically explores MDM as a non-autoregressive paradigm for end-to-end spoken dialogue. We introduce two key mechanisms: Hierarchical Block-wise Masking to mitigate training-inference distribution mismatch in block diffusion decoding, and Iterative Self-Distillation to compress multi-step refinement into few-step inference via parallel distillation. Experiments demonstrate $3.7 \times - 10 \times$ decoding speedup with 34% first-chunk latency reduction compared to AR baselines, while maintaining competitive WER and state-of-the-art text quality and speech naturalness. Our results suggest that carefully designed MDM approaches can achieve superior efficiency-quality trade-offs, opening a new paradigm for low-latency speech LLMs.

Limitations

Several aspects present opportunities for future improvement. Our training data scale remains modest compared to recent large-scale models, suggesting potential performance gains with expanded corpora. While distillation effectively reduces inference steps, quality-efficiency trade-offs become more pronounced at extremely low step counts. Speech-text alignment performance, though competitive with most baselines, leaves room for refinement through advanced optimization techniques. We also leave exploring how bidirectional context modeling affects speech quality for future work. According to results in Section 4.3, vocoder latency constitutes the dominant portion of end-to-end delay due to flow matching constraints, indicating that further system-level acceleration requires joint optimization across all components. Future work may explore larger-scale pretraining, enhanced distillation strategies, and integrated vocoder acceleration.

Ethical Considerations

All pre-trained models used in this work, including Qwen3-8B, Whisper-large-v3, and CosyVoice2, were obtained from publicly available sources and used in strict compliance with their respective licenses. The datasets employed in our experiments, including VoiceAssistant-400K and UltraChat, are publicly available and were used according to their specified terms. We did not collect any original data for this study. The speech data utilized in our experiments were either sourced from publicly available datasets or synthesized using the open-source CosyVoice2 text-to-speech model based on these datasets, minimizing potential risks related to privacy, consent, and data misuse. By relying on established, ethically sourced data and models without accessing private or sensitive information, we ensure that our research adheres to responsible AI practices throughout the development and evaluation process.

References

Marianne Arriola, Aaron Gokaslan, Justin T Chiu, Zhihan Yang, Zhixuan Qi, Jiaqi Han, Subham Sekhar Sahoo, and Volodymyr Kuleshov. 2025. Block diffusion: Interpolating between autoregressive and diffusion language models. *arXiv preprint arXiv:2503.09573*.

Jonathan Berant, Andrew Chou, Roy Frostig, and Percy Liang. 2013. Semantic parsing on freebase from

question-answer pairs. In *Proceedings of the 2013 conference on empirical methods in natural language processing*, pages 1533–1544.

Saurabhchand Bhati, Samuel Thomas, Hilde Kuehne, Rogerio Feris, and James Glass. 2025. Towards audio token compression in large audio language models. *arXiv preprint arXiv:2511.20973*.

Qian Chen, Yafeng Chen, Yanni Chen, Mengzhe Chen, Yingda Chen, Chong Deng, Zhihao Du, Ruize Gao, Changfeng Gao, Zhifu Gao, and 1 others. 2025a. Minmo: A multimodal large language model for seamless voice interaction. *arXiv preprint arXiv:2501.06282*.

Wenxi Chen, Ziyang Ma, Ruiqi Yan, Yuzhe Liang, Xiquan Li, Ruiyang Xu, Zhikang Niu, Yanqiao Zhu, Yifan Yang, Zhanxun Liu, and 1 others. 2025b. Slam-omni: Timbre-controllable voice interaction system with single-stage training. In *Findings of the Association for Computational Linguistics: ACL 2025*, pages 2262–2282.

Yushen Chen, Zhikang Niu, Ziyang Ma, Keqi Deng, Chunhui Wang, JianZhao JianZhao, Kai Yu, and Xie Chen. 2025c. F5-tts: A fairytaler that fakes fluent and faithful speech with flow matching. In *Proceedings of the 63rd Annual Meeting of the Association for Computational Linguistics (Volume 1: Long Papers)*, pages 6255–6271.

Zigeng Chen, Gongfan Fang, Xinyin Ma, Ruonan Yu, and Xinchao Wang. 2025d. dparallel: Learnable parallel decoding for dllms. *arXiv preprint arXiv:2509.26488*.

Shuang Cheng, Yihan Bian, Dawei Liu, Linfeng Zhang, Qian Yao, Zhongbo Tian, Wenhui Wang, Qipeng Guo, Kai Chen, Biqing Qi, and 1 others. 2025. Sdar: A synergistic diffusion-autoregression paradigm for scalable sequence generation. *arXiv preprint arXiv:2510.06303*.

Justin Deschenaux and Caglar Gulcehre. 2024. Beyond autoregression: Fast llms via self-distillation through time. *arXiv preprint arXiv:2410.21035*.

Ding Ding, Zeqian Ju, Yichong Leng, Songxiang Liu, Tong Liu, Zeyu Shang, Kai Shen, Wei Song, Xu Tan, Heyi Tang, and 1 others. 2025. Kimi-audio technical report. *arXiv preprint arXiv:2504.18425*.

Zhihao Du, Yuxuan Wang, Qian Chen, Xian Shi, Xiang Lv, Tianyu Zhao, Zhifu Gao, Yexin Yang, Changfeng Gao, Hui Wang, and 1 others. 2024. Cosyvoice 2: Scalable streaming speech synthesis with large language models. *arXiv preprint arXiv:2412.10117*.

Sefik Emre Eskimez, Xiaofei Wang, Manthan Thakker, Canrun Li, Chung-Hsien Tsai, Zhen Xiao, Hemin Yang, Zirun Zhu, Min Tang, Xu Tan, and 1 others. 2024. E2 tts: Embarrassingly easy fully non-autoregressive zero-shot tts. In *2024 IEEE Spoken Language Technology Workshop (SLT)*, pages 682–689. IEEE.

Xiaoran Fan, Zhichao Sun, Yangfan Gao, Jingfei Xiong, Hang Yan, Yifei Cao, Jiajun Sun, Shuo Li, Zhihao Zhang, Zhiheng Xi, Yuhao Zhou, Senjie Jin, Changhao Jiang, Junjie Ye, Ming Zhang, Rui Zheng, Zhenhua Han, Yunke Zhang, Demei Yan, and 5 others. 2025. What makes a good speech tokenizer for llm-centric speech generation? a systematic study. *Preprint*, arXiv:2506.12537.

Qingkai Fang, Shoutao Guo, Yan Zhou, Zhengrui Ma, Shaolei Zhang, and Yang Feng. 2024. Llama-omni: Seamless speech interaction with large language models. *arXiv preprint arXiv:2409.06666*.

Qingkai Fang, Yan Zhou, Shoutao Guo, Shaolei Zhang, and Yang Feng. 2025. Llama-omni2: Llm-based real-time spoken chatbot with autoregressive streaming speech synthesis. *arXiv preprint arXiv:2505.02625*.

Shansan Gong, Ruixiang Zhang, Huangjie Zheng, Jitao Gu, Navdeep Jaitly, Lingpeng Kong, and Yizhe Zhang. 2025. Diffucoder: Understanding and improving masked diffusion models for code generation. *arXiv preprint arXiv:2506.20639*.

Yuxian Gu, Li Dong, Furu Wei, and Minlie Huang. 2023. Minilm: Knowledge distillation of large language models. *arXiv preprint arXiv:2306.08543*.

Satoshi Hayakawa, Yuhta Takida, Masaaki Imaizumi, Hiromi Wakaki, and Yuki Mitsuji. 2024. Distillation of discrete diffusion through dimensional correlations. *arXiv preprint arXiv:2410.08709*.

Zhanqiu Hu, Jian Meng, Yash Akhauri, Mohamed S Aldefattah, Jae-sun Seo, Zhiru Zhang, and Udit Gupta. 2025. Accelerating diffusion language model inference via efficient kv caching and guided diffusion. *arXiv preprint arXiv:2505.21467*.

Mandar Joshi, Eunsol Choi, Daniel S Weld, and Luke Zettlemoyer. 2017. Triviaqa: A large scale distantly supervised challenge dataset for reading comprehension. In *Proceedings of the 55th Annual Meeting of the Association for Computational Linguistics (Volume 1: Long Papers)*, pages 1601–1611.

Minseo Kim, Chenfeng Xu, Coleman Hooper, Harman Singh, Ben Athiwaratkun, Ce Zhang, Kurt Keutzer, and Amir Gholami. 2025. Cdlm: Consistency diffusion language models for faster sampling. *arXiv preprint arXiv:2511.19269*.

Xuechen Li, Tianyi Zhang, Yann Dubois, Rohan Taori, Ishaan Gulrajani, Carlos Guestrin, Percy Liang, and Tatsunori B. Hashimoto. 2023. Alpacaeval: An automatic evaluator of instruction-following models. https://github.com/tatsu-lab/alpaca_eval.

Yadong Li, Jun Liu, Tao Zhang, Song Chen, Tianpeng Li, Zehuan Li, Lijun Liu, Lingfeng Ming, Guosheng Dong, Da Pan, and 1 others. 2025. Baichuan-omni-1.5 technical report. *arXiv preprint arXiv:2501.15368*.

Zijian Lin, Yang Zhang, Yougen Yuan, Yuming Yan, Jinjiang Liu, Zhiyong Wu, Pengfei Hu, and Qun Yu. 2025. Accelerating autoregressive speech synthesis inference with speech speculative decoding. *arXiv preprint arXiv:2505.15380*.

Jiaxuan Liu, Zhaoci Liu, Yajun Hu, Yingying Gao, Shilei Zhang, and Zhenhua Ling. 2025a. Diffstylelets: Diffusion-based hierarchical prosody modeling for text-to-speech with diverse and controllable styles. In *Proceedings of the 31st International Conference on Computational Linguistics*, pages 5265–5272.

Tianqiao Liu, Xueyi Li, Hao Wang, Haoxuan Li, Zhichao Chen, Weiqi Luo, and Zitao Liu. 2025b. From text to talk: Audio-language model needs non-autoregressive joint training. *arXiv preprint arXiv:2509.20072*.

Zuwei Long, Yunhang Shen, Chaoyou Fu, Heting Gao, Lijiang Li, Peixian Chen, Mengdan Zhang, Hang Shao, Jian Li, Jinlong Peng, and 1 others. 2025. Vita-audio: Fast interleaved cross-modal token generation for efficient large speech-language model. *arXiv preprint arXiv:2505.03739*.

Run Luo, Ting-En Lin, Haonan Zhang, Yuchuan Wu, Xiong Liu, Min Yang, Yongbin Li, Longze Chen, Jiaming Li, Lei Zhang, and 1 others. 2025. Openomni: Advancing open-source omnimodal large language models with progressive multimodal alignment and real-time self-aware emotional speech synthesis. *arXiv preprint arXiv:2501.04561*.

Xinyin Ma, Runpeng Yu, Gongfan Fang, and Xinchao Wang. 2025. dkv-cache: The cache for diffusion language models. *arXiv preprint arXiv:2505.15781*.

Eliya Nachmani, Alon Levkovich, Roy Hirsch, Julian Salazar, Chulayuth Asawaroengchai, Soroosh Mariooryad, Ehud Rivlin, RJ Skerry-Ryan, and Michelle Tadmor Ramanovich. 2023. Spoken question answering and speech continuation using spectrogram-powered llm. *arXiv preprint arXiv:2305.15255*.

Shen Nie, Fengqi Zhu, Chao Du, Tianyu Pang, Qian Liu, Guangtao Zeng, Min Lin, and Chongxuan Li. 2024. Scaling up masked diffusion models on text. *arXiv preprint arXiv:2410.18514*.

Shen Nie, Fengqi Zhu, Zebin You, Xiaolu Zhang, Jingyang Ou, Jun Hu, Jun Zhou, Yankai Lin, Ji-Rong Wen, and Chongxuan Li. 2025. Large language diffusion models. *arXiv preprint arXiv:2502.09992*.

OpenBMB. 2025. Minicpm-o 2.6: A gpt-4o level mllm for vision, speech, and multimodal live streaming on your phone. <https://openbmb.notion.site/185ede1b7a558042b5d5e45e6b237da9>. Accessed: 2025-12-12.

Alec Radford, Jong Wook Kim, Tao Xu, Greg Brockman, Christine McLeavey, and Ilya Sutskever. 2023. Robust speech recognition via large-scale weak supervision. In *International conference on machine learning*, pages 28492–28518. PMLR.

Takaaki Saeki, Detai Xin, Wataru Nakata, Tomoki Koriyama, Shinnosuke Takamichi, and Hiroshi Saruwatari. 2022. Utmos: Utokyo-sarulab system for voicemos challenge 2022. *arXiv preprint arXiv:2204.02152*.

Xu Wang, Chenkai Xu, Yijie Jin, Jiachun Jin, Hao Zhang, and Zhijie Deng. 2025a. Diffusion llms can do faster-than-ar inference via discrete diffusion forcing. *arXiv preprint arXiv:2508.09192*.

Yuancheng Wang, Haoyue Zhan, Liwei Liu, Ruihong Zeng, Haotian Guo, Jiachen Zheng, Qiang Zhang, Xueyao Zhang, Shunsi Zhang, and Zhizheng Wu. 2024. Maskgct: Zero-shot text-to-speech with masked generative codec transformer. *arXiv preprint arXiv:2409.00750*.

Yuhao Wang, Ziyang Cheng, Heyang Liu, Ronghua Wu, Qunshan Gu, Yanfeng Wang, and Yu Wang. 2025b. Vocalnet-m2: Advancing low-latency spoken language modeling via integrated multi-codebook tokenization and multi-token prediction. *arXiv preprint arXiv:2511.10232*.

Yuhao Wang, Heyang Liu, Ziyang Cheng, Ronghua Wu, Qunshan Gu, Yanfeng Wang, and Yu Wang. 2025c. Vocalnet: Speech llm with multi-token prediction for faster and high-quality generation. *arXiv preprint arXiv:2504.04060*.

Boyong Wu, Chao Yan, Chen Hu, Cheng Yi, Chengli Feng, Fei Tian, Feiyu Shen, Gang Yu, Haoyang Zhang, Jingbei Li, and 1 others. 2025a. Step-audio 2 technical report. *arXiv preprint arXiv:2507.16632*.

Chengyue Wu, Hao Zhang, Shuchen Xue, Shizhe Diao, Yonggan Fu, Zhijian Liu, Pavlo Molchanov, Ping Luo, Song Han, and Enze Xie. 2025b. Fast-dllm v2: Efficient block-diffusion llm. *arXiv preprint arXiv:2509.26328*.

Chengyue Wu, Hao Zhang, Shuchen Xue, Zhijian Liu, Shizhe Diao, Ligeng Zhu, Ping Luo, Song Han, and Enze Xie. 2025c. Fast-dllm: Training-free acceleration of diffusion llm by enabling kv cache and parallel decoding. *arXiv preprint arXiv:2505.22618*.

Taiqiang Wu, Chaofan Tao, Jiahao Wang, Rummung Yang, Zhe Zhao, and Ngai Wong. 2025d. Rethinking kullback-leibler divergence in knowledge distillation for large language models. In *Proceedings of the 31st International Conference on Computational Linguistics*, pages 5737–5755.

LLM-Core-Team Xiaomi. 2025. [Mimo-audio: Audio language models are few-shot learners](#).

Zhifei Xie and Changqiao Wu. 2024. Mini-omni: Language models can hear, talk while thinking in streaming. *arXiv preprint arXiv:2408.16725*.

Detai Xin, Xu Tan, Kai Shen, Zeqian Ju, Dongchao Yang, Yuancheng Wang, Shinnosuke Takamichi, Hiroshi Saruwatari, Shujie Liu, Jinyu Li, and 1 others. 2024. Rall-e: Robust codec language modeling with chain-of-thought prompting for text-to-speech synthesis. *arXiv preprint arXiv:2404.03204*.

Jin Xu, Zhifang Guo, Jinzheng He, Hangrui Hu, Ting He, Shuai Bai, Keqin Chen, Jialin Wang, Yang Fan, Kai Dang, and 1 others. 2025a. Qwen2. 5-omni technical report. *arXiv preprint arXiv:2503.20215*.

Jin Xu, Zhifang Guo, Hangrui Hu, Yunfei Chu, Xiong Wang, Jinzheng He, Yuxuan Wang, Xian Shi, Ting He, Xinfu Zhu, Yuanjun Lv, Yongqi Wang, Dake Guo, He Wang, Linhan Ma, Pei Zhang, Xinyu Zhang, Hongkun Hao, Zishan Guo, and 19 others. 2025b. Qwen3-omni technical report. *arXiv preprint arXiv:2509.17765*.

An Yang, Anfeng Li, Baosong Yang, Beichen Zhang, Binyuan Hui, Bo Zheng, Bowen Yu, Chang Gao, Chengan Huang, Chenxu Lv, and 1 others. 2025a. Qwen3 technical report. *arXiv preprint arXiv:2505.09388*.

Ling Yang, Ye Tian, Bowen Li, Xinchen Zhang, Ke Shen, Yunhai Tong, and Mengdi Wang. 2025b. Mmada: Multimodal large diffusion language models. *arXiv preprint arXiv:2505.15809*.

Jiacheng Ye, Zhihui Xie, Lin Zheng, Jiahui Gao, Zirui Wu, Xin Jiang, Zhenguo Li, and Lingpeng Kong. 2025. Dream 7b: Diffusion large language models. *arXiv preprint arXiv:2508.15487*.

Zebin You, Shen Nie, Xiaolu Zhang, Jun Hu, Jun Zhou, Zhiwu Lu, Ji-Rong Wen, and Chongxuan Li. 2025. Llada-v: Large language diffusion models with visual instruction tuning. *arXiv preprint arXiv:2505.16933*.

Aohan Zeng, Zhengxiao Du, Mingdao Liu, Kedong Wang, Shengmin Jiang, Lei Zhao, Yuxiao Dong, and Jie Tang. 2024. Gilm-4-voice: Towards intelligent and human-like end-to-end spoken chatbot. *arXiv preprint arXiv:2412.02612*.

Fengqi Zhu, Rongzhen Wang, Shen Nie, Xiaolu Zhang, Chunwei Wu, Jun Hu, Jun Zhou, Jianfei Chen, Yankai Lin, Ji-Rong Wen, and 1 others. 2025a. Llada 1.5: Variance-reduced preference optimization for large language diffusion models. *arXiv preprint arXiv:2505.19223*.

Fengqi Zhu, Zebin You, Yipeng Xing, Zenan Huang, Lin Liu, Yihong Zhuang, Guoshan Lu, Kangyu Wang, Xudong Wang, Lanning Wei, and 1 others. 2025b. Llada-moe: A sparse moe diffusion language model. *arXiv preprint arXiv:2509.24389*.

Yuanzhi Zhu, Xi Wang, Stéphane Lathuilière, and Vicky Kalogeiton. 2025c. Di [m] o: Distilling masked diffusion models into one-step generator. In *Proceedings of the IEEE/CVF International Conference on Computer Vision*, pages 18606–18618.

A Related Work

A.1 End-to-End Spoken Dialogue Systems

End-to-end spoken dialogue systems adopt two paradigms: Native Multimodal models and Aligned Multimodal models (Chen et al., 2025a).

Native multimodal models integrate understanding and generation into unified frameworks. Baichuan-Omni-1.5 (Li et al., 2025) achieves omnimodal processing via a single backbone trained on large-scale multimodal data. GLM-4-Voice (Zeng et al., 2024) leverages ultra-low bitrate tokenization and interleaved pre-training for emotive generation. Step-Audio 2 (Wu et al., 2025a) integrates Reinforcement Learning and Retrieval-Augmented Generation, while MiMo-Audio (Xiaomi, 2025) optimizes tokenization for high-density sequences. Kimi-Audio (Ding et al., 2025) unifies continuous acoustic and discrete semantic inputs, and SLAM-Omni (Chen et al., 2025b) utilizes single-stage training with grouped semantic prediction.

Conversely, Aligned Multimodal models prioritize modular alignment to preserve LLM reasoning. Qwen2.5-Omni (Xu et al., 2025a) and Qwen3-Omni (Xu et al., 2025b) adopt the Thinker-Talker architecture, with the latter further incorporating Mixture-of-Experts (MoE) for efficiency. MiniCPM-o 2.6 (OpenBMB, 2025) focuses on efficient on-device processing. For decoding, LLaMA-Omni (Fang et al., 2024) uses a Non-Autoregressive CTC decoder for low latency, whereas LLaMA-Omni 2 (Fang et al., 2025) employs an Autoregressive streaming decoder for naturalness. To reduce latency, VITA-Audio (Long et al., 2025) introduces Multiple Cross-modal Token Prediction (MCTP). VocalNet (Wang et al., 2025c) employs Multi-Token Prediction (MTP), and VocalNet-M2 (Wang et al., 2025b) augments MTP with multi-codebook tokenization.

Despite these innovations, the predominance of Autoregressive generation remains a limitation. Its strict serial dependency conflicts with the inherent redundancy of speech, inducing error accumulation and latency bottlenecks that impede the balance between responsiveness and quality.

A.2 Masked Diffusion Modeling

Masked Diffusion Modeling represents a Non-Autoregressive paradigm that breaks serial dependencies by predicting masked tokens in parallel using bidirectional context. Recent advancements have demonstrated its potential in Large Language

Models: LLaDA (Nie et al., 2025) demonstrated performance comparable to AR baselines, while subsequent scaling studies (Nie et al., 2024) established the laws for MDM. Furthermore, LLaDA 1.5 (Zhu et al., 2025a) and LLaDA-MoE (Zhu et al., 2025b) advanced alignment optimization and sparse architectures. Moreover, MDM has been successfully extended to multimodal and domain-specific tasks; LLaDA-V (You et al., 2025) and MMaDA (Yang et al., 2025b) achieve unified vision-language modeling, whereas DiffuCoder (Gong et al., 2025) and Dream 7B (Ye et al., 2025) demonstrate superior non-causal reasoning capabilities in code generation and planning.

Hybrid modeling paradigms have also attracted widespread attention. SDAR (Cheng et al., 2025) proposes a collaborative diffusion-autoregressive framework that maintains inter-block global coherence while enabling intra-block parallel decoding. Similarly, TtT (Liu et al., 2025b) integrates autoregressive text generation with non-autoregressive audio diffusion within a unified spoken dialogue system, implementing modality-specific processing mechanisms.

Despite parallel generation capabilities, MDM deployment is hindered by inference inefficiency, as optimal quality typically necessitates extensive many diffusion steps. This cumulative overhead often negates parallelization gains, making the compression of iteration steps without quality compromise a pivotal challenge.

A.3 Inference Acceleration and Distillation

To mitigate the latency overhead of diffusion decoding in MDM, researchers have primarily explored two acceleration directions: KV Cache adaptation and Knowledge Distillation.

KV Cache, while standard in Autoregressive models, poses challenges for the bidirectional attention of MDM. Fast-dLLM (Wu et al., 2025c) introduces a block-wise approximate KV Cache with confidence-aware decoding. dKV-Cache (Ma et al., 2025) proposes delayed and conditional caching strategies based on token diffusion dynamics. Furthermore, Fast-dLLM v2 (Wu et al., 2025b) and D2F (Wang et al., 2025a) efficiently convert pretrained AR models into block-diffusion frameworks compatible with standard caching mechanisms. However, while these methods enhance global throughput, they fail to address the Time to First Block. The initial block generation still necessitates a full iterative process without historical

caches, thereby impeding instantaneous responsiveness in streaming contexts.

Alternatively, Knowledge Distillation (KD) accelerates inference by compressing the multi-step refinement process. SDTT (Deschenaux and Gulcehre, 2024) employs self-distillation to match the teacher’s multi-step distribution, reducing inference steps by orders of magnitude. Di4C (Hayakawa et al., 2024) distills dimensional correlations via a hybrid student-teacher architecture. Di[M]O (Zhu et al., 2025c) achieves one-step generation by distilling masked diffusion models through an on-policy framework. CDLM (Kim et al., 2025) integrates consistency modeling with block-causal masking to reduce sampling steps. Nevertheless, these frameworks entail complex multi-model coordination. Furthermore, the extensive length of speech sequences incurs prohibitive training costs, collectively rendering existing approaches ill-suited.

B Mathematical Formulations

B.1 Sparse Semantic Anchor Alignment

We formalize the intra-block sparse semantic anchor alignment introduced in Section 3.1, which constructs an aligned semantic sequence $\mathbf{h}'_{1:T}$ from the semantic features $\mathbf{h}_{1:N}$.

Using the block partition defined in Section 3.2 with block index sets \mathcal{I}_k in Equation (5), we define the anchor positions and the corresponding assignment rule below.

Anchor position set. Within the k -th block, anchors are placed at the first Q positions. Formally, the anchor set in block k is defined as

$$\mathcal{A}_k = \{(k-1)B + q \mid q \in \{1, 2, \dots, Q\}\} \cap \mathcal{I}_k, \quad (12)$$

and the global anchor set is $\mathcal{A} = \bigcup_{k=1}^{K_{\text{blk}}} \mathcal{A}_k$, with sorted positions $\{a_1 < a_2 < \dots\}$.

Order-preserving semantic assignment. For each anchor position a_m in the sorted sequence, we assign semantic features sequentially:

$$\mathbf{h}'_{a_m} = \begin{cases} \mathbf{h}_m, & \text{if } m \leq N, \\ \mathbf{0}, & \text{if } m > N. \end{cases} \quad (13)$$

For non-anchor positions $t \notin \mathcal{A}$, we set $\mathbf{h}'_t = \mathbf{0}$.

This assignment preserves the sequential correspondence between anchor indices and semantic indices, as $a_m < a_{m'}$ implies $m < m'$.

B.2 Hierarchical Block-wise Masking Strategy

This section provides the algorithmic details of the Hierarchical Block-wise Masking strategy introduced in Section 3.2. Algorithm 1 presents the complete sampling procedure.

Expected masking ratio. Ignoring boundary effects in the final block and approximating all block lengths by B , the expected number of masked tokens can be written as

$$\mathbb{E}[|\mathcal{M}|] \approx K_{\text{blk}} \cdot \mathbb{E}[\gamma_c] \cdot B \cdot \mathbb{E}[\gamma_t]. \quad (14)$$

Comparison to Global Bernoulli masking. To characterize intermediate partially-observed states within a block, we define the intra-block masking ratio for block k as

$$R_k \triangleq \frac{|\mathcal{M} \cap \mathcal{I}_k|}{|\mathcal{I}_k|}. \quad (15)$$

For any selected block $k \in \mathcal{K}_{\text{mask}}$, Algorithm 1 samples n_k masked positions inside the block, hence $R_k = n_k/|\mathcal{I}_k|$. When $|\mathcal{I}_k| = B$ and $\gamma_t \geq 1/B$, we have $n_k = \lfloor \gamma_t B \rfloor$, which implies

$$0 \leq \gamma_t - R_k < \frac{1}{B}. \quad (16)$$

Since $\gamma_t \sim U(\gamma_t^{\min}, \gamma_t^{\max})$, the inequality above shows that, within selected blocks, training covers a family of masking ratios R_k over $[\gamma_t^{\min}, \gamma_t^{\max}]$ with resolution $1/B$. This directly matches the range of intermediate states where a block transitions from highly masked to lightly masked during block diffusion decoding.

For comparison, Global Bernoulli masking masks each token independently with probability γ_g . For any equal-length block and any $\delta > 0$, Hoeffding’s inequality and the union bound yield

$$\mathbb{P}\left(\max_{1 \leq k \leq K_{\text{blk}}} |R_k - \gamma_g| \geq \delta \mid \gamma_g\right) \leq 2K_{\text{blk}} e^{-2B\delta^2}. \quad (17)$$

This bound indicates that, as B increases, all blocks in a single sample concentrate around the same global ratio p with high probability. While this property provides uniform and comprehensive training signals suitable for foundational MDM learning, our Hierarchical Block-wise sampler explicitly induces diverse intra-block ratios R_k in selected blocks, which more directly simulates the intermediate states encountered during block diffusion decoding.

Algorithm 1 Hierarchical Block-wise Masking Sampler

Require: Sequence length T , block size B , ratio ranges $[\gamma_c^{\min}, \gamma_c^{\max}]$ and $[\gamma_t^{\min}, \gamma_t^{\max}]$
Ensure: Masked index set $\mathcal{M} \subseteq \{1, \dots, T\}$

- 1: $K_{\text{blk}} \leftarrow \lceil T/B \rceil$; $\mathcal{M} \leftarrow \emptyset$
- 2: Sample $\gamma_c \sim U(\gamma_c^{\min}, \gamma_c^{\max})$ and set $M_{\text{blk}} \leftarrow \lfloor \gamma_c \cdot K_{\text{blk}} \rfloor$
- 3: Sample $\mathcal{K}_{\text{mask}} \subseteq \{1, \dots, K_{\text{blk}}\}$ uniformly without replacement s.t. $|\mathcal{K}_{\text{mask}}| = M_{\text{blk}}$
- 4: Sample $\gamma_t \sim U(\gamma_t^{\min}, \gamma_t^{\max})$
- 5: **for** $k \in \mathcal{K}_{\text{mask}}$ **do**
- 6: $\mathcal{I}_k \leftarrow \{t \mid (k-1)B < t \leq \min(kB, T)\}$
- 7: $n_k \leftarrow \max(1, \lfloor \gamma_t \cdot |\mathcal{I}_k| \rfloor)$
- 8: Sample $\mathcal{M}_k \subseteq \mathcal{I}_k$ uniformly without replacement s.t. $|\mathcal{M}_k| = n_k$
- 9: $\mathcal{M} \leftarrow \mathcal{M} \cup \mathcal{M}_k$
- 10: **end for**
- 11: **return** \mathcal{M}

C Forward and Reverse KL for Iterative Self-Distillation

Given two distributions P_{tea} and P_{stu} defined over vocabulary \mathcal{V} , the asymmetry of KL divergence leads to fundamentally different behaviors when optimizing student parameters. The gradients of forward KL (mean-seeking) and reverse KL (mode-seeking) (Gu et al., 2023; Wu et al., 2025d) are respectively:

$$\nabla_{\theta} \text{KL}(P_{\text{tea}} \| P_{\text{stu}}) = - \sum_{v \in \mathcal{V}} P_{\text{tea}}(v) \nabla_{\theta} \log P_{\text{stu}}(v; \theta), \quad (18)$$

$$\nabla_{\theta} \text{KL}(P_{\text{stu}} \| P_{\text{tea}}) = \sum_{v \in \mathcal{V}} P_{\text{stu}}(v; \theta) \nabla_{\theta} \log \frac{P_{\text{stu}}(v; \theta)}{P_{\text{tea}}(v)}. \quad (19)$$

Forward KL is weighted by $P_{\text{tea}}(v)$, requiring the student to cover all non-zero regions of the teacher; reverse KL is weighted by $P_{\text{stu}}(v)$, allowing the student to focus on high-probability regions.

In Iterative Self-Distillation, later-step teacher predictions are typically more informative but can remain multi-modal, especially for ambiguous tokens. In this setting, reverse KL is often preferable because it encourages the student to concentrate on the teacher’s high-probability regions rather than allocating extra mass to low-probability tails, whereas forward KL tends to be

Model	KL Type	WER (%) ↓	UTMOS ↑
VocalNet-MDM (Step 4)	Forward KL	6.41	4.48
	Reverse KL	5.34	4.49
VocalNet-MDM (Step 2)	Forward KL	7.41	4.46
	Reverse KL	6.10	4.47
VocalNet-MDM (Step 1)	Forward KL	12.14	4.40
	Reverse KL	6.23	4.46

Table 5: Comparison of forward KL and reverse KL in Iterative Self-Distillation.

more mean-seeking and can over-emphasize covering all modes (Gu et al., 2023; Wu et al., 2025d).

In our task, the teacher distribution after K iterations is more refined yet retains uncertainty. Forward KL forces the student to spread mass across sub-optimal candidates where the teacher remains uncertain, while reverse KL allows the student to concentrate on regions the teacher progressively determines. From the gradient perspective, reverse KL imposes smaller penalties on low-probability regions weighted by $P_{\text{stu}}(v)$, whereas forward KL significantly penalizes even in these regions, causing resource waste. This aligns with the objective of simulating multi-step refinement in a single pass.

Table 5 compares the distillation performance of both KL variants. Results show that reverse KL achieves superior performance under low-step inference, validating its compatibility with progressive refinement tasks.

D Evaluation Details

To assess model performance, we adopt an LLM-as-a-Judge evaluation paradigm and use the evaluation prompt templates provided by OpenAudioBench (Li et al., 2025) to score model outputs in a unified manner. Our evaluation covers two task settings: open-ended generation and semi-open question answering. Specifically, the open-ended setting uses AlpacaEval, while the semi-open QA setting includes Llama Questions, TriviaQA, and Web Questions. For semi-open QA tasks, we include reference answers in the evaluation prompts to provide explicit judging criteria and to assist the judge LLM in determining the correctness of model responses. For open-ended tasks, the judge LLM assigns holistic scores according to multiple qualitative aspects, including clarity, helpfulness, relevance, accuracy, conciseness, and ease of understanding. The complete prompt designs and scoring guidelines are provided in Figures 5, 6, and 7.

Prompts for AlpacaEval

[Instruction]
 Please act as an impartial judge and evaluate the quality of the response provided by a voice assistant to the user's question displayed below. Your evaluation should consider factors such as clarity, helpfulness, relevance, accuracy, conciseness, and ease of understanding. Begin your evaluation by providing a short explanation of your reasoning. Be as objective as possible. After providing your explanation, you must rate the response on a scale of 1 to 10 by strictly following this format: '[rating]', for example: 'Rating: [[5]]'.
[Question]
 {instruction}
[The Start of Assistant's Answer]
 {response_txt}
[The End of Assistant's Answer]

Figure 5: Prompt for AlpacaEval.

Prompts for TriviaQA and Web Questions

Your will be given a question, the reference answers to that question, and an answer to be judged. Your tasks is to judge whether the answer to be judged is correct, given the question and reference answers. An answer considered correct expresses or contains the same meaning as at least ****one of**** the reference answers. The format and the tone of the response does not matter.

You should respond in JSON format. First provide a one-sentence concise analysis for the judgement in field 'analysis', then your judgment in field 'judgment'. For example,

```
"""
json
{ "analysis": "<a one-sentence concise analysis for the judgement>", "judgment": "< your final judgment, \"correct\" or \"incorrect\">"
}""
```

Question
 {instruction}

Reference Answer
 {targets}

Answer To Be Judged
 {answer_to_be_judged_text}

Figure 6: Prompt for TriviaQA and Web Questions.

Prompts for Llama Questions

Background
 You are a professional QA evaluation expert. You need to assess whether the model's answer is correct based on the standard answer.

Scoring Criteria
 Correct: The answer matches or is equivalent to the standard answer
 Incorrect: The answer is wrong or irrelevant to the question

Evaluation Guidelines
 1. The expression of answers can be flexible, not requiring exact matches. For example:
 - Numbers can be expressed in either Arabic numerals or words
 - Proper nouns can be in either English or Chinese
 - Differences in punctuation can be ignored
 2. Focus on whether the core meaning of the answer is correct

Output Format
 Provide the reasoning for your score, then generate the result in "[]" format and make sure it contains "the score is [Correct]" or "the score is [Incorrect]", for example:
 ...
 The answer is correct and equivalent to the standard answer, the score is [Correct]
 ...
 or
 ...
 The answer is incorrect and does not match the standard answer, the score is [Incorrect]
 ...

Question
 {prompt}

Standard Answer
 {gt_answer}

Model's Answer
 {answer_text}

Figure 7: Prompt for Llama Questions.